LIMNOLOGY
and
OCEANOGRAPHY

ASLO

Limnol. Oceanogr. 00, 2015, 00–00

doi: 10.1002/lno.10026

Diel cycles in the fluorescence of dissolved organic matter in dystrophic Wisconsin seepage lakes: Implications for carbon turnover

C. J. Watras,*[1,2] K. A. Morrison,[1,2] J. T. Crawford,[2] C. P. McDonald,[3] S. K. Oliver,[2] P. C. Hanson[2]

[1]Wisconsin Department of Natural Resources, Fishery and Aquatic Science Section, University of Wisconsin Trout Lake Station, Boulder Junction, Wisconsin

[2]Center for Limnology, University of Wisconsin-Madison, Madison, Wisconsin

[3]Wisconsin Department of Natural Resources, Fishery and Aquatic Science Section, Madison, Wisconsin

Abstract

We monitored the dynamics of chromophoric dissolved organic matter (CDOM) fluorescence in two Wisconsin bog lakes over timescales ranging from hours to months. Peatland-derived dissolved organic matter (DOM) was the major solute in both bog lakes, and diel cycles were dominant features of the CDOM fluorescence time series. Two distinct diel cycles that differed in amplitude and timing were observed: one in oxic epilimnia and a second in anoxic, hypolimnetic waters. These cycles were not attributable to instrumental artifacts (i.e., daily oscillations of temperature, ambient light, or battery voltage), hydrologic forcing, or the effects of inner filtering, pH, or redox conditions. High light extinction coefficients, especially in the ultraviolet region ($\sim$ 10 m^{-1} to 30 m^{-1}), suggest that DOM photolysis was negligible at the depths of the CDOM fluorescence probes in these dark-water lakes (dissolved carbon concentration: 10 mg C L^{-1} to 20 mg C L^{-1}). The diel cycles were apparently governed primarily by biological activities that mediate DOM production (release) and destruction (uptake). Rates of carbon turnover derived from properties of the epilimnetic CDOM fluorescence cycle (0.28 mg C L^{-1} d^{-1}) were similar to rates of net ecosystem production based on daily CO_2 dynamics (0.32 mg C L^{-1} d^{-1}). It appears that a small, secondary pool of labile organic carbon turns over at relatively high rates in these bog lakes, consistent with the two-compartment view of DOM stability.

Dissolved organic matter (DOM) is an important constituent of aquatic ecosystems given its role in the aquatic carbon cycle, light attenuation, metal complexation, acid–base chemistry, and microbial metabolism. Until recently, research into the quantity and quality of DOM has typically required discrete sample collection and laboratory analyses, thus limiting the temporal and spatial scale of many studies. The development of in situ optical probes that measure the absorbance or fluorescence of chromophoric dissolved organic matter (CDOM fluorescence) has enabled this component of DOM to be measured at high frequency and high resolution opening promising new avenues of research on a fundamental property of lakes and rivers. Using fluorescence probes, several investigators have observed diel CDOM cycles in freshwater environments. These cycles have been attributed to such factors as the diel entrainment of hypolimnetic waters (Gibson et al. 2001), a combination of photochemical and biologically mediated processes (Spencer et al. 2007; Saraceno et al. 2009), and the daily cycling of external hydrologic loads (Pellerin et al. 2012). Potential interactions between multiple processes currently limit interpretations of CDOM fluorescence patterns in lakes and other freshwater environments.

Diel cycles are commonly observed in freshwaters due to biological and physical rhythms that are related, either directly or indirectly, to the daily cycle of solar radiation. Specific examples include diel oscillations in pH, nitrate and other N species, metals, dissolved gases, chlorophyll *a* (Chl *a*), and stable isotopes (Nimick et al. 2011) as well as diel vertical migrations (DVM) of plankton. Many of these cycles involve or influence DOM and CDOM fluorescence. Diel cycles of CDOM fluorescence may indicate fluctuations in DOM quantity, as might result from cyclical hydrologic inputs or the biological release and uptake of DOM. Alternatively, they may result from fluctuations in the optical properties of a relatively constant pool of DOM molecules as ambient conditions change (e.g., fluorescence quench).

Although, most in situ CDOM probes cannot discriminate unequivocally between changes in DOM quantity vs. changes in DOM quality, calibration against water samples of known dissolved organic carbon (DOC) concentration can be used to quantify high frequency changes in DOM and relate them to ecosystem processes in individual lakes or rivers. For example, Spencer et al. (2012) showed that DOC

*Correspondence: cjwatras@wisc.edu

concentrations in many U.S. rivers exhibit strong linear relationships with CDOM absorbance ($r^2 \geq 0.7$), thus allowing high resolution estimates of river-specific DOM export. It is also possible to extract information on the chemical properties of DOM by measuring absorbance and/or fluorescence across multiple wavelengths, thereby assessing DOM quality on the basis of molecular weight, aromaticity, and/or origin (McKnight et al. 2001; Helms et al. 2008; Carter et al. 2012). Although these analyses are typically done in the laboratory, the deployment of multichannel in situ CDOM sensors has been advanced by Spencer et al. (2007) and Sandford et al. (2010). Given the high sensitivity of fluorescence sensors, they can potentially quantify small changes in DOM concentration that are within the measurement error of standard wet oxidation techniques (Aiken 1992).

Here, we describe the use of single channel, in situ fluorescence sensors to detect and disentangle factors potentially driving the temporal variability of DOM in dystrophic seepage lakes over timescales ranging from hours to months. We focus on seepage lakes to minimize the effect of variable hydrologic loads; and we focus on peatland-dominated lakes to emphasize the terrigenous fraction of DOM. By combining high frequency CDOM fluorescence data collected at multiple depths with ancillary limnological data and targeted field and laboratory experiments, we describe two different diel CDOM cycles and investigate relationships with ambient light intensity, temperature, pH, redox, inner filtering, and lake metabolism. We compare diel CDOM oscillations in oxic epilimnia to those in an aphotic, anoxic hypolimnion, and we investigate mechanisms that could potentially account for their differences. Finally, we explore implications with respect to internal DOM processing in peatland-dominated lakes.

Methods

Study sites

Crystal Bog and Trout Bog are small seepage lakes situated in *Sphagnum*-dominated subcatchments of the Trout Lake watershed in northern Wisconsin (46°N, 89°W). The limnological characteristics of Trout Bog are: area, 1.1 ha; maximum depth, 7.9 m; mean depth, 5.6 m; pH, 4.9 ± 0.02; ANC, 11 ± 11 μeq L^{-1}; DOC, 19.9 ± 3.6 mg C L^{-1}; conductivity, 20 ± 1.5 μS cm^{-1}; TN, 735 ± 187 μg N L^{-1}; and TP, 33 ± 21 μg P L^{-1}. For Crystal Bog they are: area, 0.5 ha; maximum depth, 2.5 m; mean depth, 1.7 m; pH, 5.2 ± 0.02; ANC, 12 ± 2 μeq L^{-1}; DOC, 10.6 ± 2 mg C L^{-1}; conductivity, 9.4 ± 1.7 μS cm^{-1}; TN, 717 ± 292 μg N L^{-1}; and TP, 19 ± 8 μg P L^{-1} (means ± standard deviation (SD) for one meter depth collected quarterly from 2000 to 2012). As there are no inflowing or outflowing streams associated with either bog lake, hydrologic inputs are limited to direct precipitation and seepage from the surrounding peatlands. Hydrologic data indicate that both bogs are typically perched above the surrounding peatland water table, but transient reversals of the hydrologic gradient between the bog and peatland occur frequently (Watras et al. 2014*a*).

DOC concentrations in both bogs are dominated by terrigenous matter derived from the surrounding peatlands. Crystal Bog is shallow and polymictic; Trout Bog is deeper and stratifies in early spring. Due to its small size, sheltered location, and relatively large mean depth, Trout Bog is strongly stratified for most of the open water season (Fig. 1). The surface mixed layer (SML) is confined to a depth of approximately one meter, but thermal stratification usually extends to the surface during daytime due to high light absorption (Fig. 1A,B). Turbulence in the SML has been attributed primarily to convection (Read et al. 2012) when warm surface waters cool and sink at night (Fig. 1B). Near the boundary between oxic and anoxic water (OA boundary, ~ 1 m to 2.5 m; Fig. 1), a series of peaks in the beam attenuation coefficient indicate a microstratified assemblage of phytoplankton and bacterioplankton (Steenbergen et al. 1989). Prior studies have shown that such microbial layers form consistently from year to year, and that they can be "hot spots" for microbially mediated processes such as sulfate reduction and methylmercury accumulation (Watras and Bloom 1994).

CDOM fluorescence monitoring

Three submersible CDOM fluorometers were deployed in the bogs: (1) a C3 Fluorometer from TurnerDesigns, (2) a C7 Cyclops Fluorometer also from TurnerDesigns, and (3) a SeaPoint Fluorometer from SeaPoint Sensors. Fluorescence specifications for the SeaPoint sensor were: Ex 370 nm center wavelength (CWL), 12 nm full width at half maximum wave height (FWHM); Em 440 nm CWL, 40 nm FWHM. Fluorescence specifications for the C3 and C7 were: Ex 340 nm CWL, 110 nm FWHM; Em 470 nm CWL, 60 nm FWHM. In addition to CDOM fluorescence, the C3 fluorometer had two additional sensors that simultaneously monitored Chl *a* (Ex : Em, 465 : 696 nm) and phycocyanin (Ex : Em, 590 : 630 nm) fluorescence.

The CDOM fluorescence sensors were deployed from buoys moored near the center of each bog (Watras et al. 2014*a*). The instrumentation buoys (roughly 1.2 m × 1.7 m) provided 12 VDC power, data-logging capability and radio communication. In Crystal Bog, a single fluorometer was deployed at a depth of 0.5 m. In Trout Bog, the three fluorometers were deployed at the midpoint of the nominal SML (0.5 m), at the middle of the anoxic hypolimnion (four meter) and near the bottom of the hypolimnion (six meter) to track high frequency dynamics in biogeochemically distinct zones of the lake. Data were logged continuously at 10 min to 30 min intervals and transmitted to the UW Trout Lake Station via radio twice daily. All CDOM fluorescence data were corrected for temperature quench and reported as $CDOM_{20}$ (i.e., CDOM fluorescence referenced to a standard temperature of 20°C: Watras et al. 2011, 2014*b*). To prevent signal degradation due

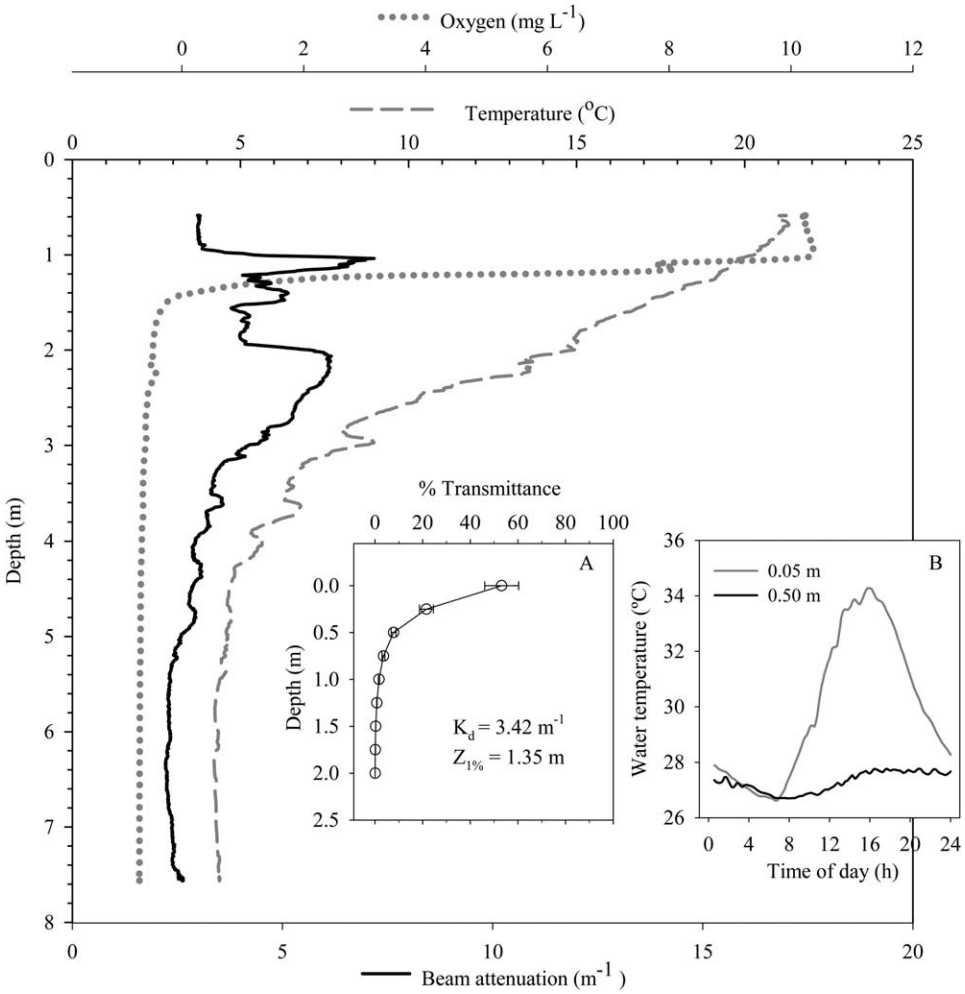

Fig. 1. The fine-scale physical structure of the Trout Bog water column during August as determined using a SeaBird™19-Plus CTD that collected data at a rate of 4 Hz as the unit was lowered through the water column at a rate of 1 cm s^{-1} to 2 cm s^{-1} (Watras, unpubl. data). Inserts: (A) ambient solar light transmission (PAR) during July and August (mean ± standard error (SE)). (B) Time series for water temperature at 0.05 m and 0.5 m during a typical midsummer day (30 min sampling intervals). Down-welling solar irradiance levels and temperature profiles were obtained from the NTL-LTER and GLEON databases maintained by the Center for Limnology, University of Wisconsin-Madison (http://lter.limnology.wisc.edu).

to fouling, the C3 fluorometer was equipped with an automatic wiper; the other two fluorometers were cleaned manually in the field each week. For codeployment in Trout Bog, the output from all three fluorometers was scaled to a common reference sample of Trout Bog water.

Ancillary measurements

DOC was determined on water samples filtered through, 0.45 μm filters into acid-washed, precombusted glass vials with Teflon lined screw caps. Organic carbon in the filtered samples was analyzed by combustion on a Shimadzu TOC-V-csh Total Organic Carbon Analyzer. Continuous measurements of PCO_2 were made in the field using a Vaisala GMM220 nondispersive infrared sensor wrapped in a watertight but gas-permeable sleeve (Johnson et al. 2010). The measurement range of the sensor was 0 μmol mol^{-1} to 5000 μmol mol^{-1}. During field deployments, the sensor output was logged hourly as the average of 60 determinations.

Experimental

A laboratory experiment was conducted to assess the effect of CO_2-driven pH quench on CDOM fluorescence. A six liter Pyrex beaker was filled with four liter of epilimnetic water from Trout Bog leaving a two liter head-space with a small vent (~ 1 cm^2). The beaker was placed on a nonreflective, black surface to minimize the back-scatter. The water was first sparged with N_2 and then bubbled with CO_2 gas (2.5%, balance air). After ~ 15 min of bubbling with CO_2, the water was again sparged with N_2. CDOM fluorescence (C7 Cyclops) and PCO_2 (Vaisala) were recorded continuously at five seconds intervals along with pH (glass combination electrode designed for low ionic strength waters)

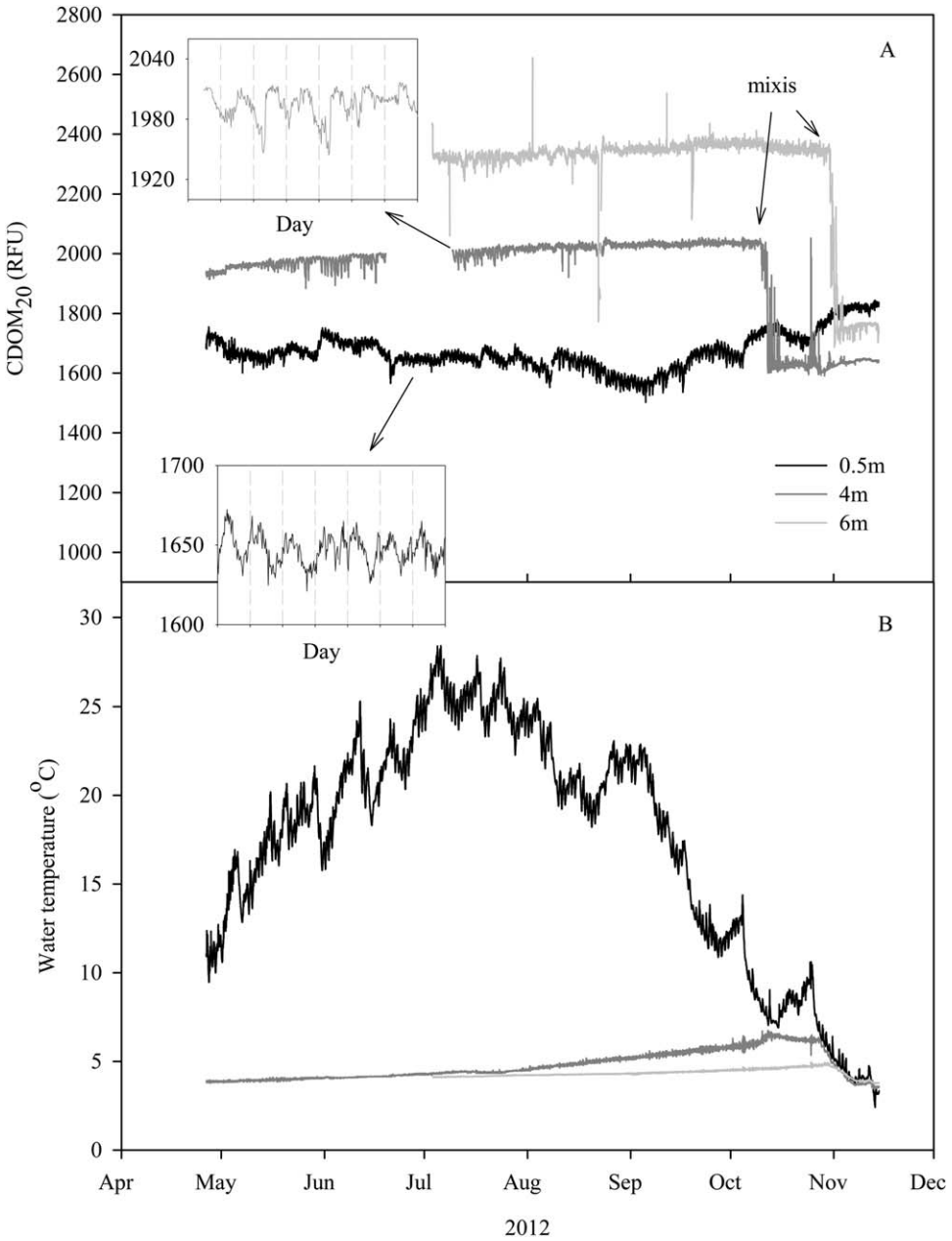

Fig. 2. Time series for (A) $CDOM_{20}$ and (B) and temperature at three depths in Trout Bog. Sampling interval 30 min. Inserts illustrate diel $CDOM_{20}$ cycle during one week time segments at 0.5 m and 4 m. $CDOM_{20}$ is the temperature-corrected fluorescence scaled to a common reference water sample (Watras et al. 2011, 2014*b*). RFU: relative fluorescence units.

and temperature. Discrete determinations of PCO_2 were made periodically using a headspace equilibration method (Striegl et al. 2012). Water for CO_2 analysis was collected with a polypropylene syringe fitted with a three-way stopcock. Fifteen milliliter of bubble-free water was passed through a 0.45 μm Whatman GMF filter and a needle into a sealed 37 mL serum bottle with N_2 headspace. Serum bottles were pretreated with two grams KCl to inhibit microbial activity (Striegl et al. 2001). CO_2 was analyzed from the serum headspace on a Shimadzu gas chromatograph (model GC-2014).

Results

The diel $CDOM_{20}$ cycle

Daily cycles of CDOM fluorescence were evident at all three depths in Trout Bog (Figs. 2–4). Spectral analysis confirmed that a 24 h periodicity dominated all three time series

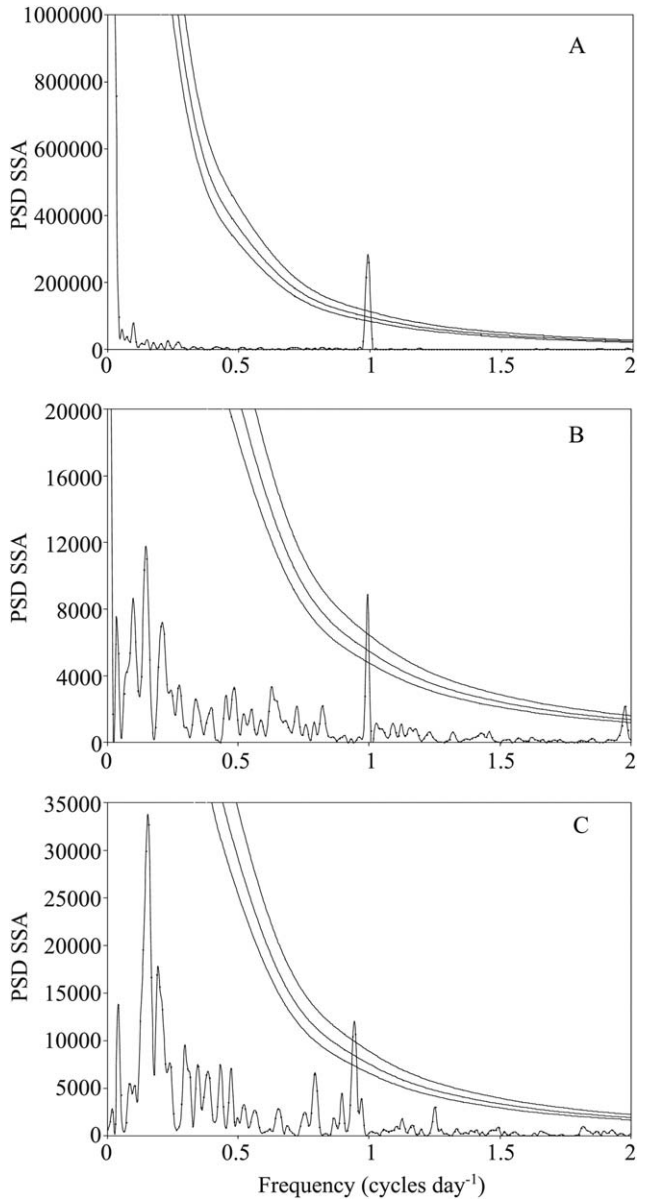

Fig. 3. Spectral analysis (fast Fourier transform, FFT) of the time series for $CDOM_{20}$ at three depths in Trout Bog during the 93 d time period from 09 July 2012 to 10 October 2012 (*see* Fig. 2). Data detrended; cs2Hann window; PSD SSA: power spectral density as sum squared amplitude. Lines indicate the 95%, 99%, and 99.9% significance levels (red noise model).

(> 99% significance level, Fig. 3). The amplitude of the diel cycle was largest in the epilimnion, and there was a distinct difference between the epilimnion and hypolimnion in the timing and shape of the oscillation (Fig. 4). In the epilimnion, CDOM fluorescence increased at night and declined during daylight in a quasi-sinusoidal pattern. In contrast, CDOM fluorescence was relatively constant at night in the hypolimnion and it increased gradually to a daytime maximum that occurred at about noon. The hypolimnetc $CDOM_{20}$ cycle is intriguing because it resembles the solar cycle even though there was no measurable light–dark cycle or diel temperature fluctuation at these depths (Figs. 1A, 2B). The presence of a diel oscillation absent an environmental cue suggests that a downward transport mechanism related to cyclical processes in or near the SML may be involved (*see* below).

It was not possible to relate the diel changes in CDOM fluorescence directly to DOC concentration at an hourly timescale due logistical and analytical constraints. Long-term data for Trout Bog indicate that duplicate DOC analyses differ on average by 0.49 ± 0.59 mg C L^{-1} (mean ± SD, n = 271 duplicate analyses from 1985 to 2012; http://lter.limnology.wisc.edu). Given a calibration factor of approximately 96 relative fluorescence units (RFU) per mg C L^{-1} for Trout Bog (from Fig. 5) and given diel oscillations ranging from 26.6 RFU to 10.4 RFU in the field (from Fig. 4), a daily oscillation in DOC concentration would not be discernable. Although, this constraint limits generalization from CDOM fluorescence to DOC at subdaily timescales, we note that CDOM fluorescence tracked DOC concentration reasonably well at coarser temporal and spatial scales where variability in the field was larger (e.g., Fig. 5A, r^2 = 0.43).

Below we discuss several mechanistic hypotheses that might explain the observed oscillations in DOM fluorescence, and we evaluate potential drivers in the context of ancillary experiments, additional field data, and prior published studies.

Discussion

Underlying mechanisms

Potential artifacts

At least three instrumental artifacts could potentially generate a diel oscillation in CDOM fluorescence independent of DOC concentration: (1) interference by ambient light, (2) residual error in the temperature compensation algorithm, and (3) cyclical fluctuations in the power source. The ambient light hypothesis was tested in Crystal Bog by codeploying two CDOM fluorescence sensors, one of which was outfitted with a flow-through light shield. The results showed that the same diel $CDOM_{20}$ cycle was evident with both sensors (Watras et al. 2011). Likewise, the diel $CDOM_{20}$ cycle was also observed to persist in the Trout Bog hypolimnion despite the absence of measurable light (cf., Figs. 1, 3, and 4). The hypolimnetic $CDOM_{20}$ cycle also occurred in the absence of diel temperature fluctuations, arguing against residual error in the temperature compensation algorithm as an explanation (Fig. 2B). Finally, although the supply voltage from batteries fluctuated daily due to the solar charging unit on the buoys, the daily oscillation from ~ 12.5 V at night to ~ 14.5 V during daylight was not in phase with the $CDOM_{20}$ cycle. More importantly, the electronic output of the fluorometers was well regulated. For example, the SeaPoint fluorometer gives 5 V ± 10 mV output over an input

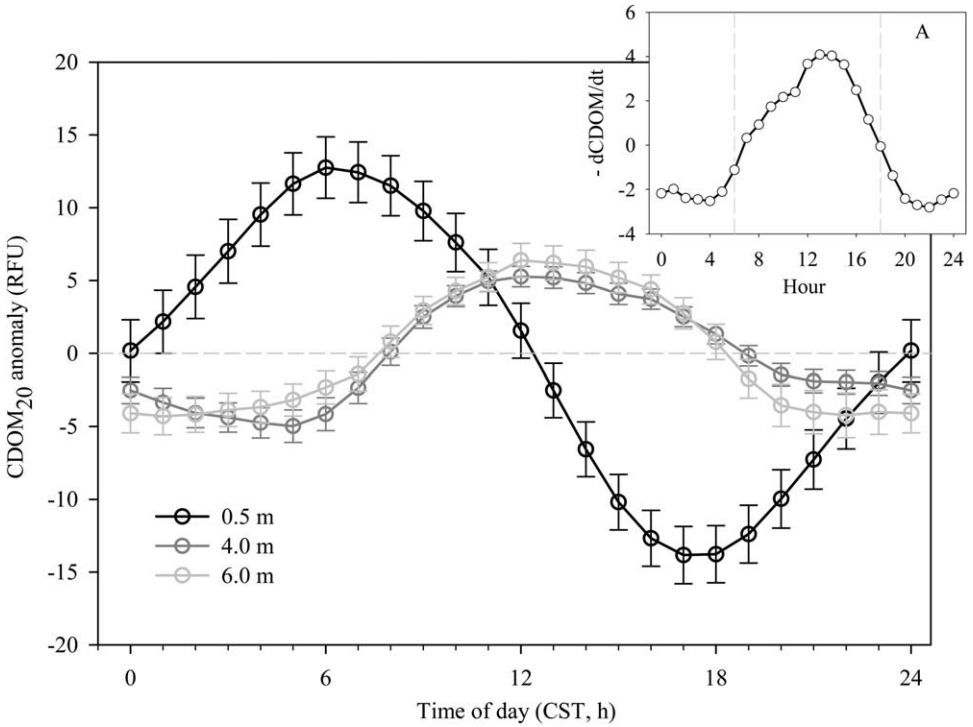

Fig. 4. Average diel $CDOM_{20}$ anomalies at three depths in Trout Bog. Data are three hours centered moving averages (detrended) ± SE for each hour of the day over the 52 d time period 09 July 2012 to 30 August 2012. Mean wave height of anomalies (peak to trough): 26.6 RFU at 0.5 m, 10.2 RFU at 4 m, and 10.7 RFU at 6 m. Insert A shows derivative of $CDOM_{20}$ cycle at 0.5 m.

range of 5.5 V to 20 V (Jeff Mather, SeaPoint Sensors, personal communication). These observations indicate that diel $CDOM_{20}$ cycling in the two bogs did not result from any of these three instrumental artifacts.

Inner filtering constitutes another form of artifact that can interfere with fluorescence signals by absorbing or scattering excitation or emitted light within the sensing volume of a probe. The inner filter effect damps a fluorescence signal and typically causes nonlinearity in the relationship between fluorescence intensity and fluorophore concentration. The effect can be strong under conditions of high turbidity or high fluorescent substrate concentrations (Downing et al. 2012).

The relationship between CDOM fluorescence and DOC concentration was previously shown to be nonlinear for Trout Bog water due to inner filtering as DOC increased from $\sim$ 0 mg C L^{-1} to $\sim$ 17 mg C L^{-1} (Watras et al. 2011). However, over the relatively narrow range of concentration observed in the field ($\sim$ 17.5 ± 1 mg C L^{-1}; Fig. 5), the relationship is approximately linear. Nonetheless, evidence of an inner filter effect likely due to particles was observed in the field during a late-summer cyanophyte bloom (Fig. 6). During the bloom, there were large spikes in phycocyanin fluorescence in the epilimnion ($\sim$ 10-fold; Fig. 6A). The phycocyanin spikes, which occurred around noon each day, were too large to be attributed to cyanophyte growth or photo-adaptation, and they coincided with similarly sharp decreases in CDOM fluorescence (Fig. 6B,C). As a consequence, the diel $CDOM_{20}$ cycle at 0.5 m was damped and distorted (Fig. 6D).

The sharp spikes in phycocyanin fluorescence suggest that cyanophytes were migrating past the C3 probe at a similar time each day. Cyanophyte DVMs are well documented for freshwaters, involving buoyancy regulation via gas vesicles in response to changes in light intensity (Walsby 1994). Laboratory studies have shown that cyanophytes lose buoyancy and sink under high light intensity while at low light intensity they gain buoyancy and float up (Oliver and Walsby 1984). If this DVM pattern holds for the population in Trout Bog, our observations would suggest that a layer of cyanophytes aggregated near the C3 sensor window (0.5 m) at mid-day when solar radiation was maximum, and they subsequently floated up into near-surface water as the ambient light intensity declined. A definitive test of this hypothesis would require the deployment of additional fluorescence probes. In any case, to confirm an inner filter effect on CDOM fluorescence, we subtracted the "distorted" CDOM fluorescence cycle from the "typical" $CDOM_{20}$ cycle and compared the residual signal to the daily pattern of phycocyanin fluorescence (Fig. 7). The result indicates reasonably good agreement between the $CDOM_{20}$ disparity and the daily phycocyanin cycle (Fig. 7B), and it is consistent with an inner filter effect being exerted by the bloom. However, it

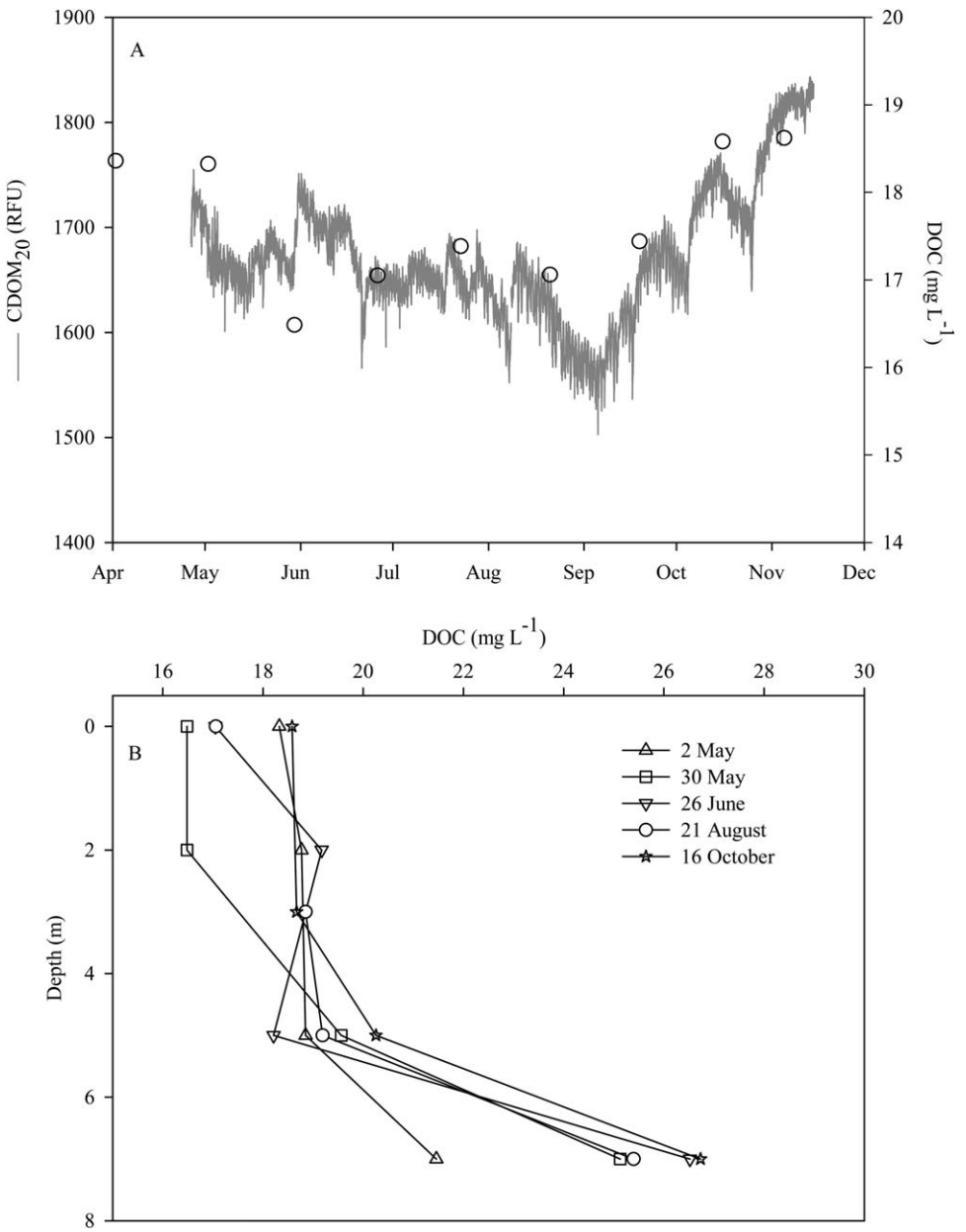

Fig. 5. (A) Comparison of time series for $CDOM_{20}$ and DOC in surface waters of Trout Bog during 2012. (B) Depth profiles of DOC in Trout Bog from May to October 2012.

in no way suggests that inner filtering underlies the typical diel CDOM cycle observed during nonbloom time periods.

Variability in DOM quality

Aside from artifacts, CDOM fluorescence is subject to other complicating factors that can affect excitation or emission signals independent of DOC concentration (Aiken 2014). Below, we evaluate the effects of pH and redox conditions, two environmental factors that could potentially account for (or contribute to) the diel $CDOM_{20}$ cycles we observed.

Light absorbance by DOM in freshwater is known to be affected by pH-driven changes in molecular conformation (Sutton and Sposito 2005; Pace et al. 2011). Absorbance by DOM chromatophores deceases with decreasing pH; and as this effect would presumably hold for fluorophores, the pH effect might account for a diel CDOM cycle especially if cyclical changes in pH resulted from CO_2 dynamics and the daily cycle of lake metabolism.

Under laboratory conditions, a very large addition of CO_2 to Trout Bog water caused a pH decline of about 0.2 units, and there was a strong positive correlation between pH and CDOM fluorescence (r^2 = 0.81; Fig. 8). Furthermore, the changes in pH and CDOM fluorescence were readily reversible. When

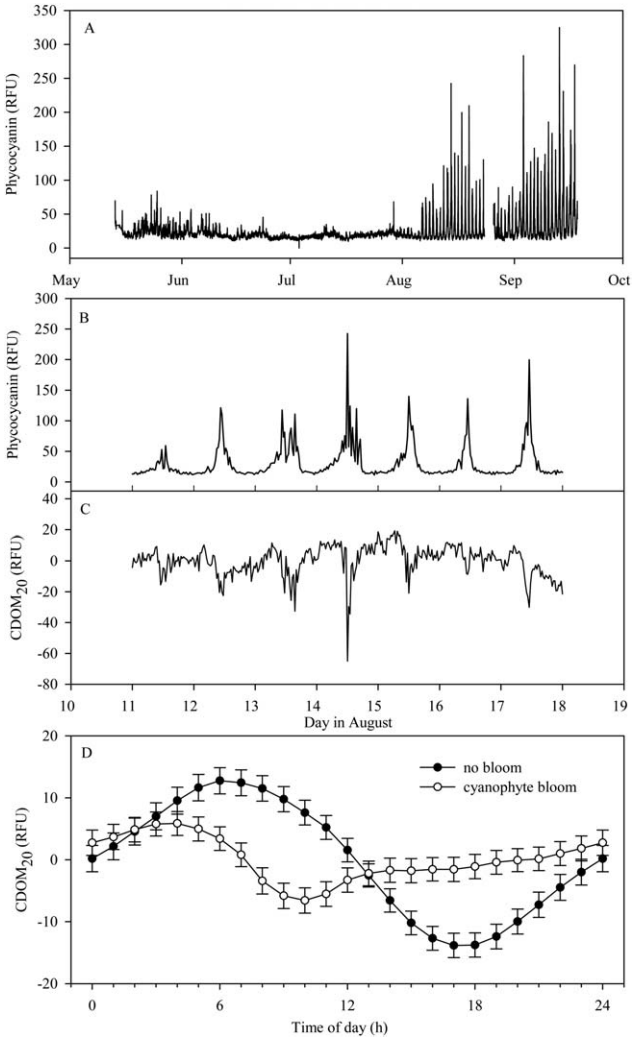

Fig. 6. Effect of cyanophyte bloom on the diel cycle of CDOM fluorescence in Trout Bog, autumn 2013. (A) Time series of phycocyanin fluorescence during open water season; (B) diel changes in phycocyanin fluorescence intensity at 0.5 m; (C) diel changes in $CDOM_{20}$ fluorescence at 0.5 m showing minima that correspond to phycocyanin maxima at approximately noon each day; (D) comparison of "typical" diel $CDOM_{20}$ fluorescence anomaly (cf., Fig. 4) to the "distorted" anomaly during cyanophyte bloom (three hours centered moving average of detrended $CDOM_{20}$ data from 06 August 2013 to 13 September 2013).

sparged with N_2 to drive off CO_2, both pH and CDOM fluorescence returned to their initial values. During the experiment, PCO_2 as determined by GC analysis was 56.9 ± 51 Pa, 407.1 ± 134 Pa, and 1761 ± 118 Pa (mean ± SD, $n = 3$) near the start, middle, and end of bubbling with 2.5% CO_2 gas. The PCO_2 returned to 23.9 ± 25.2 Pa after the N_2 sparge.

Under field conditions, the relationship between pH and CDOM fluorescence was different than observed in the lab. (1) Daily fluctuations of pH in the field were an order of magnitude smaller than we induced with a massive CO_2 injection to Trout Bog water (Fig. 9A). The small fluctuation in field pH is consistent with equilibrium modeling (PHREEQ) where the mean ambient temperature, pH, alkalinity, and a daily PCO_2 anomaly of ± 30 Pa were specified as inputs. The model predicted a pH anomaly of ± 0.01 unit, which agrees well with the field observations. (2) Contrary to expectation, the field data indicate a weak negative relationship between pH and CDOM fluorescence rather than the positive correlation observed in the lab. The correlation coefficient ($r = 0.45$) and tilted oval shape of the plot shown on Fig. 9D resemble the relationship expected for two diel cycles that are out of phase by approximately eight hours ($r = \cos\Delta\varphi$, where $\Delta\varphi$ is the difference in phase angle (or lag); cf., Lissajous curve, Gray 1999). (3) There was an unexpected strong positive correlation between PCO_2 and CDOM fluorescence rather than the negative correlation observed in the lab (Fig. 9E, $r^2 = 0.88$). We note that the CDOM fluorescence signal was affected by a cyanophyte bloom during this time period (cf., Figs. 7, 8); but with this caveat, the field data suggest that PCO_2 and CDOM fluorescence in the field may be related, not due to a pH effect but potentially reflecting a link to lake metabolism (*see* below).

Oxidation–reduction potential is another environmental factor that can affect DOM fluorescence. Quinone-like moieties are a ubiquitous component of terrigenous DOM and several studies indicate that quinone fluorescence varies with redox state (Fulton et al. 2004; Cory and McKnight 2005; Miller et al. 2006). During summer in Trout Bog, dissolved O_2 concentrations in the epilimnion have historically averaged ~ 80% of saturation, varying on a daily timescale by ~ 20% due to diel changes in the balance between photosynthesis and respiration (http://lter.limnology.wisc.edu). Given the constant presence of O_2 in the SML, one would not expect the redox potential to vary by more than few mV (Wetzel 2001) likely with negligible effect on quinone fluorescence.

Although, there is a strong redox gradient across the metalimnion of Trout Bog, the hypolimnion is permanently anoxic during summer (Fig. 1). Given the stability of physical conditions deep in the hypolimnion (Figs. 1, 2B), one would also expect relatively constant redox conditions at 4 m and 6 m. But anaerobic microbial activity can exert a direct effect on the redox state of quinones via electron shuttling. Several lines of evidence indicate that Fe(III)-reducers can transfer electrons to quinones which then abiotically transfer the electrons back to Fe(III)-oxides (Scott et al. 1998; Lovley and Blunt-Harris 1999). However, inducing a sustained diel fluorescence cycle this way would require proximity to a source of Fe(III), a suitable electron donor (e.g., fermentation by-products) and a diel cycle of microbial activity. To satisfy the first two of these requirements, Fe(III)-reducers typically occupy zones near the OA boundary above the zone of sulfate reduction. Given the shallow location of the OA boundary in Trout Bog and evidence that microbial stratification is clustered at depths between ~ 1 m and 2.5 m (Fig. 1), it seems unlikely that a diel cycle of electron shuttling through quinones drives the hypolimnetic $CDOM_{20}$ cycle we observed.

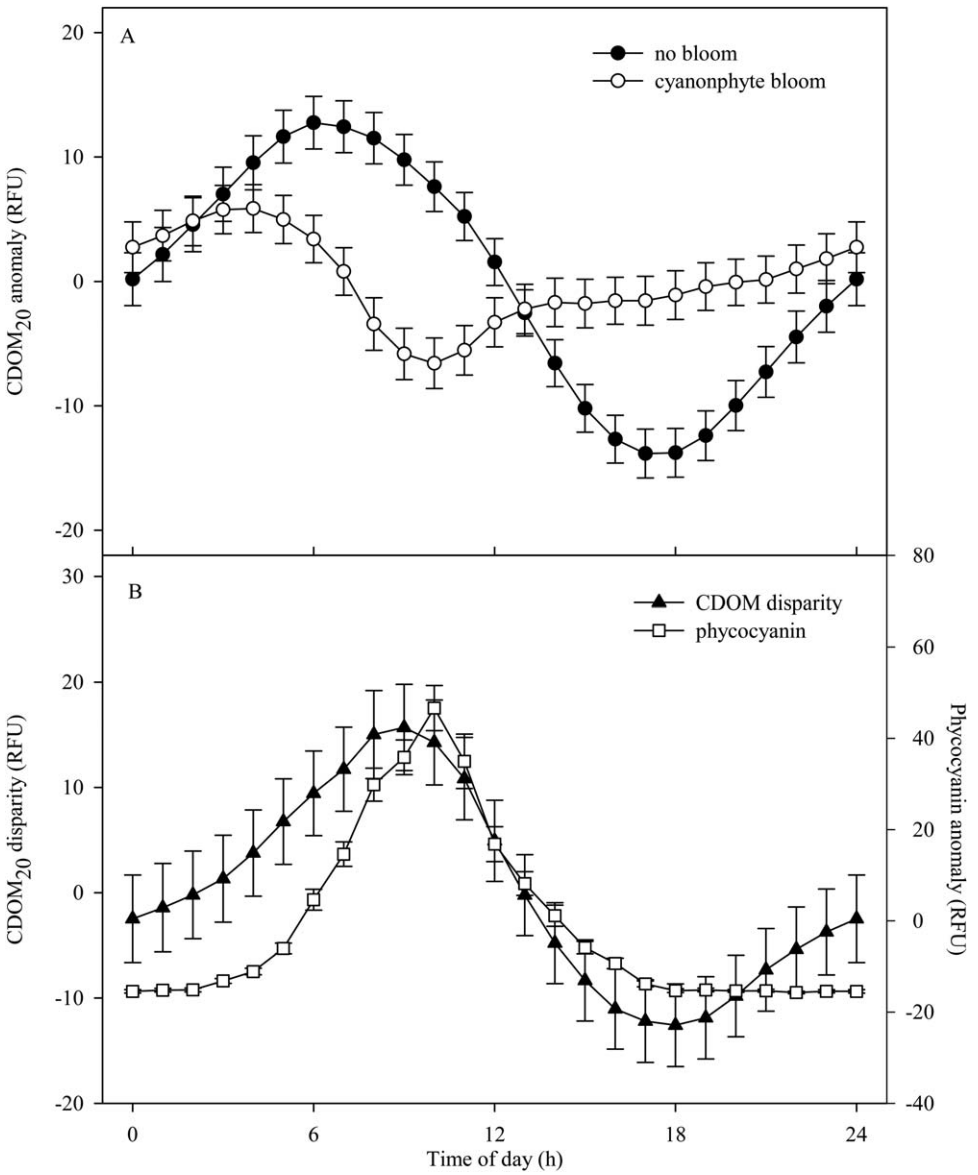

Fig. 7. Estimated inner filter effect of cyanophyte bloom on diel $CDOM_{20}$ fluorescence signal in Trout Bog. (A) Comparison of daily $CDOM_{20}$ cycles during nonbloom (09 July 2012 to 30 August 2012) and bloom (06 August 2013 to 18 September 2013) time periods. Data are detrended three hours centered moving average ± SE. (B) Daily cycle of phycocyanin fluorescence intensity compared to the difference between the two $CDOM_{20}$ cycles shown in panel (A). Phycocyanin data are the detrended three hours centered moving average ± SE (06 August 2013 to 18 September 2013).

Variability in DOM quantity

As neither instrument-related artifacts, inner filtering, pH, nor redox cycling can easily explain the diel $CDOM_{20}$ cycles observed in these bog lakes, we tentatively hypothesize that the cycles are driven by temporal imbalances between DOM production and destruction processes. These processes can be governed by solar radiation and/or by biological activity. The photolysis of DOM is generally attributed to the ultraviolet (UV) portion of the solar spectrum via reactions that can yield reactive oxygen species, DIC (photomineralization) as well as lower molecular weight organic carbon substrates (photobleaching) that support heterotrophic microbial growth (reviewed by Sulzberger and Durisch-Kaiser 2009). Because the declining phase of the epilimnetic $CDOM_{20}$ cycle in Trout Bog begins near dawn and ends near dusk (Fig. 4), and because the derivative of the $CDOM_{20}$ cycle ($-\ \delta CDOM/\delta t$) resembles the daily solar cycle (Fig. 4A), the photolysis of DOM is potentially an important driving mechanism.

In incubation experiments with water from seven Ontario lakes (DOC: 2 mg L^{-1} to 5 mg L^{-1}), Molot and Dillon (1997) derived photomineralization rate constants that ranged from

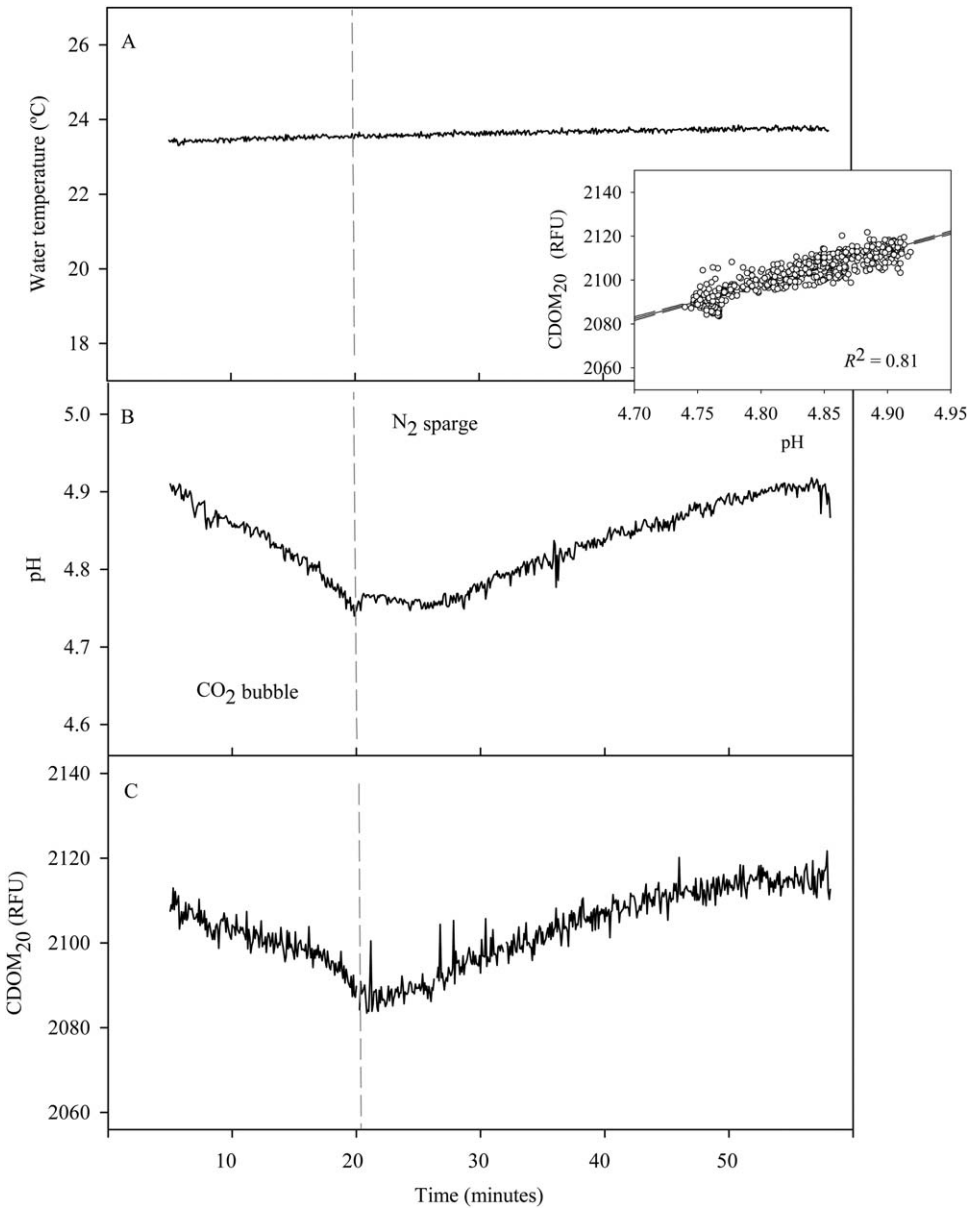

Fig. 8. Results of laboratory experiment to determine the effect of CO_2-induced pH change on $CDOM_{20}$ fluorescence in a sample of Trout Bog water.

0.002 d^{-1} to 0.008 d^{-1} under a solar UV flux that averaged 400 kJ m^{-2} d^{-1}. These daily rates implied relatively high DOM turnover during the estimated 214 d of ice-free conditions. DOM replenishment in the lakes was attributed to inflow via tributary streams. As photolysis rates declined with increasing DOC, presumably due to UV extinction, Molot and Dillon surmised that nonphotolytic decay might be relatively more important in high DOC lakes such as Crystal Bog and Trout Bog.

During midsummer at Trout Bog, incident photosynthetically active radiation (PAR) under clear-sky conditions averages approximately 10 MJ m^{-2} d^{-1}, and given a solar UV : PAR ratio of $\sim$ 0.04 from Molot and Dillon (1997), the incident UV flux would be similar to experimental conditions with Ontario lake waters ($\sim$ 400 kJ m^{-2} d^{-1}). However, light extinction within Trout Bog is high (K_{d_PAR} = 3.42 m^{-1}; Fig. 1A) so only 8% of the incident PAR reaches the CDOM fluorescence sensor at 0.5 m. Attenuation in the UV region is substantially greater, as evidenced by the well-known exponential increase in absorbance by DOM at wavelengths below 400 nm. Although, spectroradiometric data for Trout Bog are not available, the spectral distribution of downwelling light (300 nm to 850 nm) has been measured in three nearby dystrophic lakes with similarly high DOC concentrations

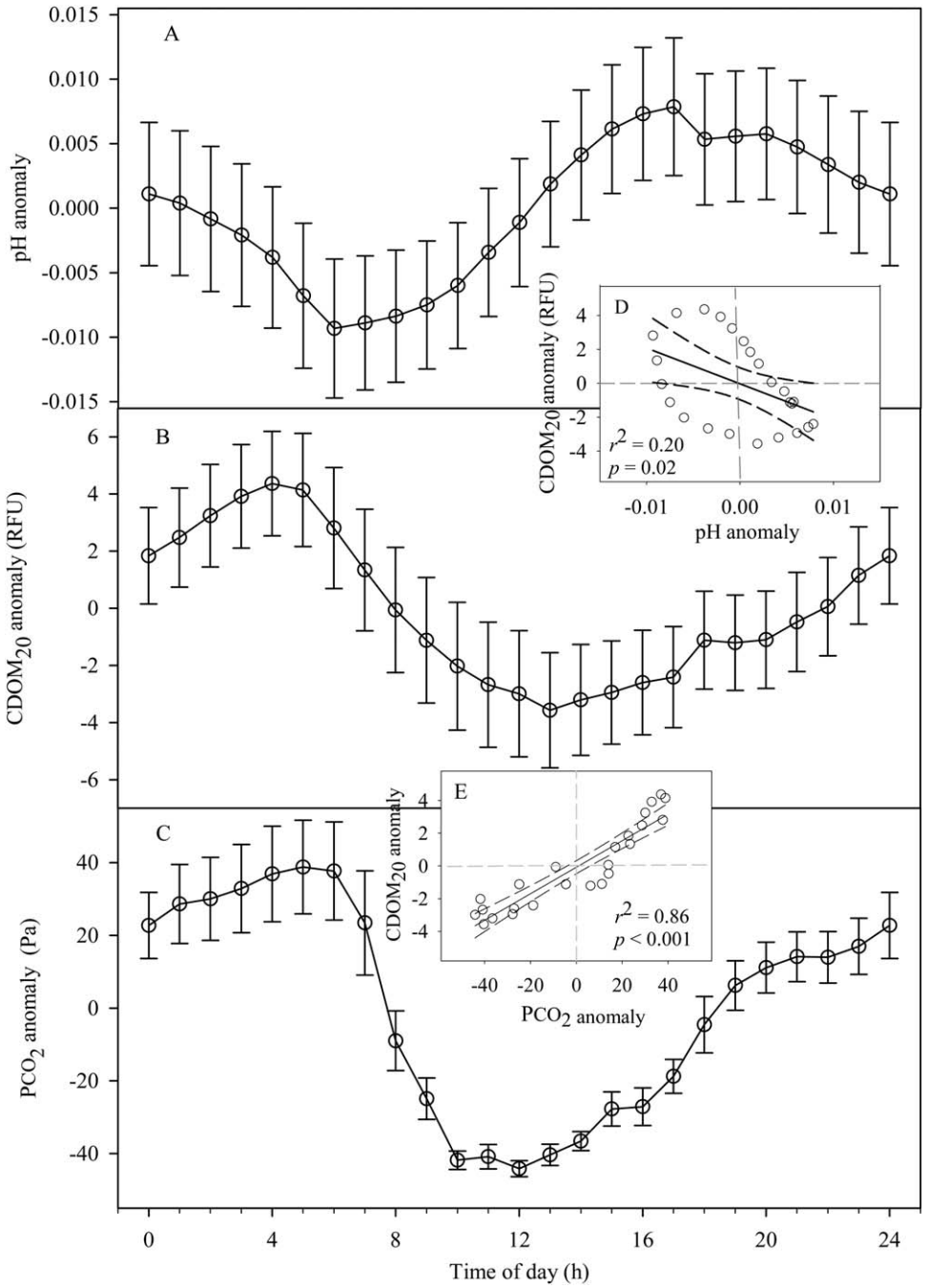

Fig. 9. Diel anomalies of (A) pH, (B) $CDOM_{20}$, and (C) PCO_2 under field conditions with sensors colocated at a depth of ~ 0.5 m in Trout Bog during a one week time period (28 August 2013 to 05 September 2013). Hourly pH and $CDOM_{20}$ are the centered moving average (seven hours, detrended) ± SE. Hourly PCO_2 sensor output was corrected to 25°C and 1013 hPa (daily PCO_2 for the week averaged 63.4 Pa). (D) Relationship between pH and $CDOM_{20}$. (E) Relationship between PCO_2 and $CDOM_{20}$.

(16 mg C L^{-1} to 21 mg C L^{-1}; Watras and Baker 1988). In all three lakes, downwelling radiation at wavelengths less than 440 nm was approximately 0.04 μE m^{-2} s^{-1} nm^{-1} at 0.5 m water depth (roughly five orders of magnitude lower than surface irradiance). A similarly low estimate of UV penetration is obtained by applying the broadband UVA attenuation coefficient (θ) of Scully and Lean (1994), where $\theta_{UVA} = 4\ 0.299[DOC]^{1.53}$ yielding $\theta_{UVA} = 24.9\ m^{-1}$ at a DOC concentration of 18 mg C L^{-1}. Estimated this way, the UV flux at 0.5 m in Trout Bog would be only 1.6 J m^{-2} d^{-1}.

Although, the low UV irradiance flux at 0.5 m in Trout Bog has negligible photolytic potential, the incident solar

Table 1. Estimates of organic carbon turnover in bog lakes based on diel $CDOM_{20}$ cycling.

Bog	Layer	Estimated rate (d^{-1})*	Time (d)†	Turnover (% yr^{-1})
Trout Bog	Epilimnion	0.016	180	288
	Hypolimnion	0.002	180	36
	Whole lake	0.0045	180	81
Crystal Bog	Whole lake	0.006	180	108

*Derived from diel $CDOM_{20}$ cycle as explained in text. Sign changes with time of day. Net rate = zero for stationary time-series where DOM production and destruction balance during 24 h.
†Open water time period.

UV flux of 400 kJ m^{-2} d^{-1} would be sufficient to photodegrade DOM in water very near the surface. Convective mixing of photodegraded near-surface water might then cause a periodic decline in the $CDOM_{20}$ signal at 0.5 m. However, near-surface waters heat up during daylight (reaching temperatures exceeding 34°C) and convective mixing within the epilimnion occurs when surface water cools at night (Fig. 1B). Thus, although the near-surface photolysis of DOC may be an important process in the lake as a whole, the daily entrainment cycle of photodepleted near-surface water would be the opposite of that needed to account for the observed daytime decline of CDOM fluorescence. Interestingly, however, the nocturnal entrainment of DOM from the shallow metalimnion would be consistent with the observed night-time increase in CDOM fluorescence (Fig. 4).

With respect to biological degradation, the major pool of DOM in bog lakes is generally acknowledged to be recalcitrant on the order of years to decades (Wetzel 2001), but the rapid biological turnover of a smaller labile DOM pool is consistent with a two-compartment view of stability as described by Sutton and Sposito (2005). Coupled cycles of DOM production and consumption are widely recognized for marine waters, constituting the well-known microbial loop (Azam et al. 1983). In bog waters, daily changes in either phase of the microbial loop (release or uptake) would superimpose a diel signal on the larger, relatively stable pool of terrigenous DOM.

As with photolysis rates, existing estimates of DOM turnover due to microbiological processes have been derived largely from bottle incubation experiments. One of the first studies was conducted at sea by Kirchman et al. (1991) who measured DOM loss during shipboard incubation of 0.8 μm filtered seawater (to remove zooplankton and phytoplankton) in the dark. Decay rate constants from this study (0.025 d^{-1} to 0.363 d^{-1}) had a profound effect on estimates of the age of organic carbon in the ocean. More recent experiments that link microbial and photolytic DOM decay in freshwater and coastal environments suggest similarly high rates (De Lange et al. 2003; Nieto-Cid et al. 2006). On the production side, substantial DOM accumulation due to phytoplankton excretion has been quantified in studies such as those of Romera-Castillo et al. (2010) who estimated carbon specific rates of 0.09 μg C μg C^{-1} d^{-1} to 0.12 μg C μg C^{-1} d^{-1} during the exponential growth of axenic phytoplankton cultures. These experiments also demonstrated that the released DOM was fluorescent.

Comparable calculations for Trout Bog based on the average wave height of the $CDOM_{20}$ cycle (peak to trough) yield an apparent rate constant of 0.016 d^{-1} in the epilimnion (given an amplitude of ± 13.3 RFU around a mean value of 1633 RFU; Fig. 4). In the anoxic, aphotic hypolimnion (4 m and 6 m) the $CDOM_{20}$ pool was larger (2323 RFU on average) and the amplitude of oscillation was smaller (± 5.2 RFU, Fig. 4) yielding a rate constant of 0.002 d^{-1}. This range of rates (0.002 d^{-1} to 0.016 d^{-1}) is remarkably similar to the range of DOM turnover estimates reported in previous studies of temperate and boreal freshwaters using other approaches (summarized by Hanson et al. 2011).

Turnover rates expressed in units of carbon can be approximated using our calibration factor of 96 RFU mg C^{-1} L^{-1} and the magnitude of diel $CDOM_{20}$ oscillations (26.6 RFU d^{-1} and 10.4 RFU d^{-1} from Figs. 4, 5). The quotients are 0.28 mg C L^{-1} d^{-1} for the epilimnion and 0.11 mg C L^{-1} d^{-1} for the hypolimnion of Trout Bog. As a check on the value for the epilimnion, we can use the PCO_2 time series from Fig. 9C to estimate free water metabolism assuming quasi-equilibrium conditions over a series of days, such that

$$\delta CO_2/\delta t = GPP - R + F_{atm} = 0 \quad (1)$$

where GPP is gross primary production, R is respiration and F_{atm} is the atmospheric CO_2 flux. For the Trout Bog epilimnion, we estimate that CO_2 at saturation would be roughly 39 Pa or 1.83 mg C L^{-1} (based on a gas transfer velocity (k) = 0.43 m d^{-1}, SML depth = 1.53 m (both from Read et al. 2012), temperature (T) = 20°C, and the Henry's constant (k_H) = 0.39). Comparison with the observed mean daily PCO_2 of 63.4 Pa or 2.97 mg C L^{-1} (Fig. 9 legend) indicates that the epilimnion is supersaturated by about 1.14 mg C L^{-1} on average. As net ecosystem production (NEP) equals (GPP – R), we can rearrange Eq. 1 to show that $F_{atm} = -NEP$. In other words, estimating the atmospheric CO_2 flux is the same as estimating net ecosystem productivity. Then, as $F_{atm} = (k_H \times C_{supersaturation})/SML\ depth = (0.43\ m\ d^{-1} \times 1.14\ g\ C\ m^{-3})/1.53\ m = 0.32\ g\ C\ m^{-3}\ d^{-1}$, we find that NEP = −0.32 mg C L^{-1} d^{-1} (similar to the rate we estimated above (0.28 mg C L^{-1} d^{-1}) based on the magnitude of the diurnal $CDOM_{20}$ oscillation). We emphasize that these rates are hypothetical and apply only to the epilimnion.

Integrated over the entire water column during the open water period, our best estimate of DOM turnover in Trout Bog based on the diel $CDOM_{20}$ cycle is equivalent to 81% yr^{-1} of the average pool of DOM in the lake (Table 1). This value is higher than estimates of DOC biomineralization

based on recent equilibrium modeling (16% to 28% yr^{-1}, Hanson et al. 2014). For the shallower, polymictic Crystal Bog, estimated DOM turnover for the whole lake is relatively higher than in Trout Bog, whether based on modeling (38% to 68% yr^{-1}, Hanson et al. 2014) or on the diel $CDOM_{20}$ cycle (108% yr^{-1}, Table 1).

We tentatively conclude that internal DOM processing underlies the diel $CDOM_{20}$ oscillations observed in these dystrophic lakes. Because light attenuation is strong, especially at UV wavelengths, we hypothesize that the principle factor driving the oscillations is biological activity rather than photolysis. This hypothesis is supported by estimates of free water metabolism based on dissolved CO_2 dynamics. Our findings suggest that a small pool of DOM cycles rapidly despite the apparent constancy of DOM concentrations over long timescales. However, the identification of specific mechanisms remains to be done.

The difference between epilimnetic and hypolimnetic $CDOM_{20}$ cycling in Trout Bog is intriguing but it also remains unexplained (Fig. 4). Given the shape of the oscillations and absence of diel cues at 4.0 m and 6.0 m depth, a physical linkage presumably exists between the hypolimnion and an adjacent system that is directly influenced by the solar cycle. Two hypothetical mechanisms that could link surface and deep waters are (1) the DVM of zooplankton and (2) diel fecal pellet production. DVMs between anoxic and oxic waters are well documented for *Chaoborus* larvae, and *Chaoborus* have been observed during the day in the anoxic hypolimnion of Trout Bog (Rahel and Waymire Nutzman 1994). Sloppy feeding after upward migration at night followed by excretion at depth during daytime could produce the requisite coupling between $CDOM_{20}$ cycles. Rapid microbial uptake of the released DOM could complete the cycles at all depths. The settling of particulate organic matter also could provide a linkage between the epilimnetic and hypolimnetic waters. Because the $CDOM_{20}$ cycles at 4.0 m and 6.0 m are in phase, the linkage would have to be due to fast-settling particles. Living phytoplankton cells typically settle slowly, < 1 m d^{-1}, and even large (> 64 μm) organic carbon particles only settle at 2–3 m d^{-1} (Burns and Rosa 1980). However, zooplankton fecal pellets settle rapidly, often > 100 m d^{-1} (Smayda 1969); and they can lose up to 20% of their carbon content during the first hour following expulsion via leakage (Møller et al. 2003). Given the relatively short timescales over which pellet settling and DOC leakage occur, it is possible (albeit speculative) that they constitute a pathway by which a diel signal expressed in surface waters (zooplankton feeding) is concurrently replicated at depth.

References

Aiken, G. 1992. Chloride interference in the analysis of dissolved organic carbon by the wet oxidation method. Environ. Sci. Technol. **26**: 2435–2439. doi:10.1021/es00036a015

Aiken, G. 2014. Fluorescence and dissolved organic matter: A chemist's perspective. In P. Coble, J. Lead, A. Baker, D. Reynolds and R. G. M. Spencer [eds.], Aquatic organic matter fluorescence. Cambridge Univ. Press.

Azam, F., T. Fenchel, J. G. Field, J. S. Gray, L.-A. Meyer-Reil, and F. Thingstad. 1983. The ecological role of water-column microbes in the sea. Mar. Ecol. Prog. Ser. **10**: 257–263. doi:10.3354/meps010257

Burns, N. M., and F. Rosa. 1980. In situ measurement of the settling velocity of organic carbon particles and 10 species of phytoplankton. Limnol. Oceanogr. **25**: 855–864. doi:10.4319/lo.1980.25.5.0855

Carter, H. T., E. Tipping, J.-F. Koprivnjakb, M. P. Miller, B. Cookson, and J. Hamilton-Taylor. 2012. Freshwater DOM quantity and quality from a two-component model of UV absorbance. Water Res. **46**: 4532–4542. doi:10.1016/j.watres.2012.05.021

Cory, R. M., and D. M. McKnight. 2005. Fluorescence spectroscopy reveals ubiquitous presence of oxidized and reduced quinines in dissolved organic matter. Environ. Sci. Technol. **39**: 8142–8149. doi:10.1021/es0506962

De Lange, H. J., D. P. Morris, and C. E. Williamson. 2003. Solar UV photodegredation of DOM may stimulate freshwater food webs. J. Plankton Res. **25**: 111–117. doi:10.1093/plankt/25.1.111

Downing, B. D., B. A. Pellerin, B. A. Bergamaschi, J. F. Saraceno, and T. E. C Kraus. 2012. Seeing the light: The effects of particles, dissolved materials, and temperature in in situ measurements of DOM fluorescence in rivers and streams. Limnol. Oceanogr.: Methods **10**: 767–775. doi:10.4319/lom.2012.10.767

Fulton, J. R.; D. M. McKnight; C. Foreman, R. Cory, C. Stedmon, E. Blunt. 2004. Changes in fulvic acid redox state through the oxycline of a permanently ice-covered Antarctic lake. Aquat. Sci. **66**: 27–46. doi:1015-1621/04/010027-20

Gibson, J. A. E., W. F. Vincent, and R. Pienitz. 2001. Hydrologic control and diel photobleaching of CDOM in a subarctic lake. Arch. Hydrobiol. **152**: 143–159.

Gray, A. 1999. Modern differential geometry of curves and surfaces with Mathematica, 2nd ed. CRC Press.

Hanson, P. C., I. Buffam, J. A. Rusak, E. H. Stanley and C. Watras. 2014. Quantifying lake allochthonous organic carbon budgets using a simple equilibrium model. Limnol. Oceanogr. **59**: 167–181. doi:10.4319/lo.2014.59.01.0167

Hanson, P. C., D. P. Hamilton, E. H. Stanley, N. Preston, O. C. Langman, and E. L. Kara. 2011. Fate of allochthonous dissolved organic carbon in lakes: A quantitative approach. PloS One **6**: 1–12. doi:10.1371/journal.pone.0021884

Helms, J. R., A. Stubbins, J. D. Ritchie, E. C. Minor, D. J. Kieber, and K. Mopper. 2008. Absorption spectral slopes, and slope ratios as indicators of molecular weight, source, and photobleaching of chromophoric dissolved organic matter. Limnol. Oceanogr. **53**: 955–969. doi:10.4319/lo.2008.53.3.0955

Johnson, M. S., M. F. Billett, K. J. Dinsmore, M. Wallin, K. E. Dyson, and R. S. Jassal. 2010. Direct and continuous measurement of dissolved carbon dioxide in freshwater aquatic systems—method and applications. Ecohydrology **3**: 68–78. doi:10.1002/eco.95

Kirchman, D. L., Y. Suzuki, C. Garside, and H. Ducklow. 1991. High turnover rates of organic carbon during a spring phytoplankton bloom. Nature **352**: 612–614. doi:1038/352612a0

Lovley, D. R., and E. L. Blunt-Harris. 1999. Role of humic-bound iron as an electron transfer agent in dissimilatory Fe(III) reduction. Appl. Environ. Microbiol. **65**: 4252–4254.

McKnight, D. M., E. W. Boyer, P. K. Westerhoff, P. T. Doran, T. Kulbe, and D. T. Andersen. 2001. Spectrofluorometric characterization of dissolved organic matter for indication of precursor organic material and aromaticity. Limnol. Oceanogr. **46**: 38–48. doi:10.4319/lo.2001.46.1.0038

Miller, M. P., D. M. McKnight, R. M. Cory, M. W. Williams, and R. L. Runkel. 2006. Hyporheic exchange and fulvic acid redox reactions in an alpine stream/wetland ecosystem, Colorado Front Range. Environ. Sci. Technol. **40**: 5943–5949. doi:10.1021/es060635j

Møller, E. F., P. Thor, and T. G. Nielsen. 2003. Production of DOC by Calanus finmarchicus, C. glacialis and C. hyperboreus through sloppy feeding and leakage from fecal pellets. Mar. Ecol. Prog. Ser. **262**: 185–191. doi:10.3354/meps262185

Molot, L. A., and P. J. Dillon. 1997. Photolytic regulation of dissolved organic carbon in northern lakes. Global Biogeochem. Cycles **11**: 357–365. doi:10.1029/97GB01198

Nieto-Cid, M., X. A. Alvarez-Salgado, and F. F. Perez. 2006. Microbial and photochemical reactivity of fluorescent dissolved organic matter in a coastal upwelling system. Limnol. Oceanogr. **51**: 1391–1400. doi:.

Nimick, D. A., C. H. Gammons, and S. R. Parker. 2011. Diel biogeochemical processes and their effect on the aqueous chemistry of streams: A review. Chem. Geol. **238**: 3–17. doi:10.1016/j.chemgeo.2010.08.017

Oliver, R. L., and A. E. Walsby. 1984. Direct evidence for the role of light-mediated gas vesicle collapse in the bouyancy regulation of *Anabaena flos-aquae* (cyanobacteria). Limnol. Oceanogr. **29**: 879–886. doi:10.4319/lo.1984.29.4.0879

Pace, M. L., I. Reche, J. J. Cole, A. Fernández-Barbero, I. P. Mazuecos, and Y. T. Prairie. 2011. pH change induces shifts in the size and light absorption of dissolved organic matter. Biogeochemistry **108**: 109–118. doi:10.1007/s10533-011-9576-0

Pellerin, B. A., J. F. Saraceno, J. S. Shanley, S. D. Sebestyen, G. R. Aiken, W. M. Wolheim, and B. A. Bergamaschi. 2012. Taking the pulse of snowmelt: In situ sensors reveal seasonal, event and diel patterns of nitrate and organic matter variability in an upland forest stream. Biogeochemistry **108**: 183–198. doi:10.1007/s10533-011-9589-8

Rahel, F. J., and J. Waymire Nutzman. 1994. Foraging in a lethal environment: Fish predation in hypoxic water of a stratified lake. Ecology **75**: 1246–1253. doi:10.2307/1937450

Read, J. S., and others. 2012. Lake-size dependency of wind shear and convection as controls on gas exchange. Geophys. Res. Lett. **39**: L09405. doi:10.1029/2012GL051886

Romera-Castillo, C. H. Sarmento, X. A. Alvarez-Salgado, J. M. Gasol, and C. Marrase. 2010. Production of chromophoric dissolved organic matter by marine phytoplankton. Limnol. Oceanogr. **55**: 446–454. doi:10.4319/lo.2010.55.1.0446

Sandford, R. C., R. Bol, and P. J. Worsfold. 2010. In situ determination of dissolved organic carbon in freshwaters using a reagentless UV sensor. J. Environ. Monit. **12**: 1678–1683. doi:10.1039/c0em00060d

Saraceno, J. F., B. A. Pellerin, B. D. Downing, E. Boss, P. A. M. Bachand, and B. A. Bergamaschi. 2009. High-frequency in situ optical measurements during a storm event: Assessing relationships between dissolved organic matter, sediment concentrations, and hydrological processes. J. Geophys. Res. **114**: G00F09. doi:10.1029/2009JG000989

Scott, D. T., D. M. McKnight, E. L. Blunt-Harris, S. E. Kolesar, and D. R. Lovley. 1998. Quinone moieties act as electron acceptors in the reduction of humic substances by humics-reducing microorganisms. Environ. Sci. Technol. **32**: 2984–2989. doi:10.1021/es980272q

Scully, N. M., and D. R. S. Lean. 1994. The attenuation of ultraviolet radiation in temperate lakes. Arch. Hydrobiol. Beih. **43**: 135–144.

Smayda, T. J. 1969. Some measurements of the sinking rate of fecal pellets. Limnol. Oceanogr. **14**: 621–625.

Spencer, R. G. M., K. D. Butler, and G. R. Aiken. 2012. Dissolved organic carbon and chromophoric dissolved organic matter properties of rivers in the U.S.A. J. Geophys. Res.: Biogeosci. **117**: G03001. doi:10.1029/2011JG001928

Spencer, R. G. M., B. A. Pellerin, B. A. Bergamaschi, B. D. Downing, T. E. C. Kraus, D. R. Smart, R. A. Dahlgren, and P. J. Hernes. 2007. Diel variability in riverine dissolved organic matter composition determined by in situ optical measurements in the San Joaquin River (California, USA). Hydrolog. Process. **21**: 3181–3189. doi:10.1002/hyp.6887

Steenbergen, C. L. M., H. J. Korthals, A. L. Baker, and C. J. Watras. 1989. Microscale vertical distribution of algal and bacterioplankton in Lake Vechten. FEMS Microbiol. Ecol. **62**: 209–220. doi:10.1111/j.1574-6968.1989.tb03695.x

Striegl, R. G., M. M. Dornblaser, C. P. McDonald, J. R. Rover, and E. G. Stets. 2012. Carbon dioxide and methane emissions from the Yukon River system. Global Biogeochem. Cycles **26**: GB0E05. doi:10.1029/2012GB004306

Striegl, R. G., P. Kortelainen, J. P. Chanton, K. P. Wickland, G. C. Bugna, and M. Rantakari. 2001. Carbon dioxide partial pressure and ^{13}C content of north temperate and boreal lakes at spring ice melt. Limnol. Oceanogr. **46**: 941–945. doi:10.4319/lo.2001.46.4.0941

Sulzberger, B., and E. Durisch-Kaiser. 2009. Chemical characterization of dissolved organic matter (DOM): A prerequisite for understanding UV-induced changes of DOM absorption properties and bioavailability. Aquat. Sci. **71**: 104–126. doi:10.1007/s00027-008-8082-5

Sutton, R., and G. Sposito. 2005. Molecular structure in soil humic substances: A new view. Environ. Sci. Technol. **39**: 9009–9015. doi:10.1021/es050778q

Walsby, A. E. 1994. Gas vesicles. Microbiol. Rev. **58**: 94–144.

Watras, C. J., and A. L. Baker. 1988. The spectral distribution of downwelling light in northern Wisconsin Lakes. Arch. Hydrobiol. **112**: 481–494. doi:10.1007/BF00007935

Watras, C. J., and N. S. Bloom. 1994. The vertical distribution of mercury species in Wisconsin lakes: Accumulation in plankton layers, p. 137–152. In C. J. Watras and J. W. Huckabee [eds.], Mercury pollution: Integration and synthesis. Lewis Publishers.

Watras, C. J., P. C. Hanson, T. L. Stacy, K. M. Morrison, J. Mather, Y.-H. Hu, and P. Milewski. 2011. A temperature compensation method for CDOM fluorescence sensors in freshwater. Limnol. Oceanogr.: Methods **9**: 296–301. doi:10.4319/lom.2011.9.296

Watras, C. J., M. Morrow, K. Morrison, S. Scannell, S. Yaziciaglu, J. S. Read, Y.-H. Hu, P. C. Hanson, and T. Kratz. 2014a. Evaluation of wireless sensor networks (WSNs) for remote wetland monitoring: Design and initial results. Environ. Monit. Assess. **186**: 919–934. doi:10.1007/s10661-013-3423-8

Watras, C. J., K. M. Morrison, J. Mather, P. Milewski, and P. C. Hanson. 2014b. Correcting CDOM fluorescence for temperature effects under field conditions in freshwaters. Limnol. Oceanogr.: Methods **12**: 23–24. doi:10.4319/lom.2014.12.23

Wetzel, R. G. 2001. Limnology: Lake and river ecosystems. Academic Press.

Acknowledgments

The authors thank Jeff Rubsam for excellent technical support in the field and laboratory, and we thank Gosia Golub for use of the Vaisala model GMM220 PCO_2 module.

Support was provided by the Wisconsin Department of Natural Resources, the Wisconsin Focus on Energy Program and by the US National Science Foundation (Northern Temperate Lakes – Long-term Ecological Research Program, Grant No. DEB-0822700). This paper is a joint contribution from the Fisheries and Aquatic Science Section, Wisconsin Department of Natural Resources and from the Trout Lake Research Station, Center for Limnology, University of Wisconsin-Madison.

Submitted 2 May 2014
Revised 14 October 2014
Accepted 31 October 2014

Associate editor: Peter Hernes